Semiconductor Physics, Quantum Electronics & Optoelectronics, 2023. V. 26, No 4. P. 388-397.

Semiconductor physics

Nanomechanical properties of polycrystalline vanadium oxide thin films of different phase composition

P.M. Lytvyn[*], V.M. Dzhagan, M.Ya. Valakh, A.A. Korchovyi, O.F. Isaieva, O.A. Stadnik, O.A. Kulbachynskyi, O.Yo. Gudymenko, B.M. Romanyuk, V.P. Melnik

V. Lashkaryov Institute of Semiconductors Physics, NAS of Ukraine, 03680 Kyiv, Ukraine
[*]Corresponding author e-mail: plyt@isp.kiev.ua

Abstract. Vanadium oxide (VO_x) thin films are promising materials, exhibiting electrical, optical, and mechanical properties highly tunable by processing and structure. This work uniquely applying atomic force microscopy (AFM) nanoindentation correlated with X-ray diffractometry and Raman spectroscopy structural analysis to investigate the intricate connections between VO_x post-annealing, phase composition, and resulting nanoscale mechanical functionality. Utilizing an ultra-sharp diamond tip as a nanoscale indenter, indentation is performed on VO_x films with systematic variations in structure – from mixed insulating oxides to VO_2-dominated films. Analytical modeling enables extraction of hardness and elastic modulus with nanoscale resolution. Dramatic mechanical property variations are observed between compositions, with order-of-magnitude increases in hardness and elastic modulus for the VO_2-rich films versus insulating oxides. Ion implantation further enhances nanomechanical performance through targeted defect engineering. Correlating indentation-derived trends with detailed structural and morphological characterization elucidates explicit structure-property relationships inaccessible by other techniques. The approach provides critical mechanics-driven insights into links between VO_x synthesis, structure evolution, and property development. Broader implementation will accelerate processing optimization for electronics and advanced fundamental understanding of nanoscale structure-functionality relationships.

Keywords: polycrystalline vanadium oxide thin films, phase composition, atomic force microscopy, nanoindentation, X-ray diffraction, Raman spectroscopy, defect engineering, ion implantation.

https://doi.org/10.15407/spqeo26.04.388
PACS 62.20.de, 68.37.Ps, 68.60.Bs, 68.55.Ln, 78.30.j, 81.40.Jj

Manuscript received 12.10.23; revised version received 31.10.23; accepted for publication 22.11.23; published online 05.12.23.

1. Introduction

Vanadium oxides (VO_x) are renowned for their diverse electronic and optical properties, positioning them as potential candidates for advanced electronic applications. Among these, VO_2 is particularly noteworthy due to its metal-insulator transition (MIT) around 68 °C, which is concomitant with a structural phase transformation [1–3]. This sharp MIT in VO_2 not only paves the way for ultra-fast switching in field-effect transistors and data storage devices but also qualifies it as an efficient thermo-chromic material. These properties cover applications like bolometers and thermally adjustable filters in infrared sensing [4–6]. V_2O_3 is another member of the vanadium oxide family, also exhibits MIT, making it a potential material for neuromorphic computing systems that emulate biological neural networks [7, 8]. The transition temperature of both VO_2 and V_2O_3 can be fine-tuned by doping with elements such as W, Mo and Ti, optimizing their performance in various devices [9, 10].

Magnéli phases, including V_4O_7 and V_6O_{13}, are metallic vanadium oxides known for their high electrical conductivity. Their potential as low-resistance electrodes in VLSI circuits (Very-Large-Scale Integration) and as thermoelectric materials are currently being explored [11–13]. Furthermore, amorphous vanadium oxides, represented as VO_{2+x}, are becoming popular in resistive memory devices due to their inherent memristive properties [14–16]. Beyond these, vanadium oxides also are known to be applicable to smart windows, e-paper displays, and Li-ion batteries [17, 18].

Investigating the mechanical parameters of electronic materials provides vital insights into the complex relationship between atomic structures, defects

and overall material behavior [19, 20]. In the case of vanadium oxide, the main factor in these properties is the crystal structure. Different polymorphic structures, including monoclinic VO_2, orthorhombic V_2O_5 or various amorphous phases, can greatly impact the material hardness and elasticity [21–28]. It's noteworthy that even within the same VO_2 phase, temperature-induced polytype transformations lead to an abrupt increase in the elasticity modulus of VO_2 – up to approximately 17 GPa – during the phase transition from the isolating monoclinic to the metallic rutile phase [29]. For polycrystalline thin films, the size and distribution of the crystalline grains are also significant determinants of material properties. Smaller grain sizes result in higher hardness. Moreover, the properties and behavior of the grain boundaries themselves can also impact the material overall mechanical behavior. The composition of vanadium oxide, in terms of stoichiometry and the incorporation of dopants, can dramatically influence mechanical properties. Changes in the vanadium-to-oxygen ratio, or the addition of other elements, can induce alterations in the crystal structure, defect behavior and electronic structure. All these changes can, in turn, affect both the hardness and elasticity of this material.

Ion beam processing is recognized as a technique that facilitates systematic adjustments to the structural order, charge carrier interactions, resistive switching, and optical absorption features of VO_x thin films [29]. Through ion implantation, there is the capability for precise manipulation by the atomic-scale structure and attributes of vanadium oxide thin films. Subjecting VO_x to high-energy ion beams introduces defects and dopants, which in turn modify the material crystalline structure, electronic band configuration, electrical conductivity, and optical transmissivity. These radiation-induced damage and lattice doping interfere with electron mobility and metal-insulator transitions, while concurrently altering optical bandgaps [30–32]. It is pertinent to examine how these structural alterations manifest in the nanomechanical properties of thin vanadium oxide films. Yet, there is a lack of information regarding these effects in VO_x films.

Therefore, this work employs AFM-based nano-indentation [33, 34] to investigate the nanomechanical properties of magnetron-sputtered VO_x thin films of different phase compositions, both post-annealed in various atmospheres and modified by ion beam irradiation. The high localization and force sensitivity of AFM nanoindentation enables delineation of variations in nanomechanical performance arising from crystalline phase and irradiation-induced defects in the complex functional oxide films. Relating measured nanomechanical trends to structural and functional properties will provide critical insights into the structure-property relationships in this technologically important class of electronic materials. The aim is to demonstrate the efficacy of AFM nanoindentation for express estimation of the multiphase balance and structural defects in VO_x thin films, to facilitate process optimization and performance improvements for electronics applications. The results will also provide further fundamental understanding of the links between structure evolution and nanoscale mechanical behavior in post-processed and ion beam engineered oxide thin films.

2. Experimental details

Preparation of the vanadium oxide thin-film samples was performed following the methodology established in our group's prior studies [35–39]. Specifically, the films were deposited on Si substrates using magnetron sputtering from a VO_2 target, with the current of 70 μA, 250 V bias, and the substrate temperature set to 200 ± 5 °C. Throughout the sputtering, the pressure in the chamber was maintained at ~10^{-6} Torr. The resulting film thickness ranged between 100…200 nm. Post-deposition, the samples underwent thermal annealing at the temperatures 300…450 °C for 15 min in an N_2 environment. A parallel set of samples was annealed in an oxygen-rich atmosphere, serving as reference samples to accurately identify various V_xO_y compounds within the VO_2 films. Some of the VO_2/Si films were subjected to Ar^+ ion implantation at the energy 180 keV and the dosage $4.4 \cdot 10^{14}$ ions/cm². The process was carried out at the current density 0.1 mA/cm². This treatment resulted in a nearly uniform distribution of microdeformations and defects throughout the depth of the VO_2 film.

The NanoScope IIIa Dimension 3000 scanning probe microscope was used to study the surface topography and nano-mechanical testing of the V_xO_y films. The tapping mode of an atomic force microscope (AFM) and the ultra-sharp silicon tips were used for topography measurements. The nanoindentation mode and the cube corn diamond indenter with the apex radius 50 nm (135 N/m spring constant) were used for hardness and elasticity measurements.

Raman spectra were excited with 457 nm emission of a solid-state laser and acquired using a single-stage spectrometer MDR-23 (LOMO) equipped with a cooled CCD detector (Andor iDus 420, UK). The laser power density on the samples was less than 10^3 W/cm^2, to preclude any thermal or photo-induced modification of the samples. A spectral resolution did not exceed 4 cm^{-1} for all excitation radiation wavelengths and was determined from the Si phonon peak width of a single crystal Si substrate. The crystal structure of the VO_x films was analyzed using an X'Pert ProMPD X-ray diffractometer, employing the CuK_α radiation with a wavelength of $\lambda = 0.15418$ nm.

3. Results and discussion

Upon examining the surfaces of the oxygen-reach annealed V_xO_y films (Figs 1a, 1b), we observed a relatively uniform distribution (with a root mean square (RMS) roughness close to 3.5 nm) featuring scarcely detectable nano-grains and micron-sized blocks, which were separated by nanopores and depressed boundaries. Contrastingly, the nanocrystalline surfaces produced by annealing in an argon environment (Figs 1c, 1d)

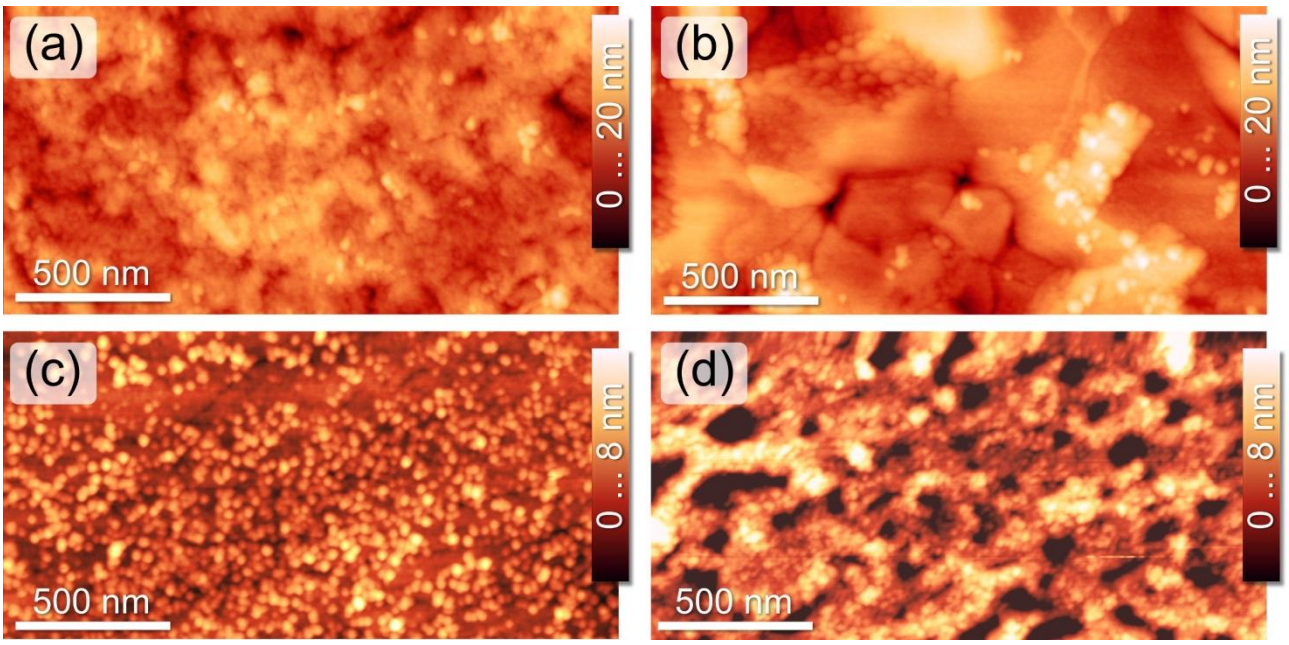

Fig. 1. AFM images of V_xO_y films annealed in the oxygen-reach (a, b) and in the inert atmosphere (c, d). The annealing temperatures were 300 °C (a), 400 °C (b), 400 °C (c), and 450 °C (d).

demonstrated a significant decrease in grain sizes from approximately 50 to 20 nm, as the annealing temperature was increased from 400 to 450 °C. It is noteworthy that there were some dips observed at higher temperatures (the black spots in (d)), which led to an increase in the RMS value from 1.4 up to 2.1 nm.

To characterize the nanomechanical properties of V_xO_y films, we gathered numerous load-penetration (L-P) curves at 11, 15, and 20 μN load levels. These curves were collected from diverse surface areas with the lateral spacing 2 μm. Fig. 2 shows a representative set of L-P curves for the annealed V_xO_y films. We used the Hertz and Oliver–Pharr fits to depict the purely elastic and elastoplastic behavior of the films under indentation, respectively [34, 40, 41].

The Hertz model assumes that the material is isotropic, linearly elastic, and that the contact area is much smaller than the tip radius. The Hertz model for a spherical indenter is given by

$$F = \frac{3}{4} E^* \sqrt{r_{tip}} \left(h - h_0\right)^{1.5}, \qquad (1)$$

where F is the loading force, E^* is the reduced modulus, r_{tip} is the indenter tip radius, and $h - h_0$ is the penetration depth. The reduced modulus E^* is related to Young's modulus E and the Poisson ratio ν by $E^* = E/\left(1-\nu^2\right)$. The fitting parameters include the reduced modulus E^* and the contact point h_0, and these are applicable only during the initial phase of indentation (*e.g.*, penetration depth 5…10 nm).

For larger penetration depths, the Hertz contact model may be insufficient. Therefore, we employed the Oliver–Pharr model, an extension of the Hertz model that incorporates plastic deformation. This model presumes the material to be isotropic and that the deformation reaches complete plasticity at the maximum load. The model is based on the approximation of the unloading curve by a power law: $F = \alpha\left(h - h_f\right)^m$. Here, h_f represents the final displacement after complete unloading, while α and m are material-dependent constants. With the known area function of the indenter A and the initial slope S of the unloading curve, we can determine the hardness H and elastic modulus E of the material as follows:

$$H = \frac{E_{\max}}{A}, \qquad (2)$$

$$E^* = \sqrt{\frac{\pi}{2}} \frac{S}{\sqrt{A}}. \qquad (3)$$

As observed in Fig. 2, the oxygen-reach annealed samples exhibit remarkably low hardness, with the tip penetrating to a depth of over half the film thickness. This suggests a significant influence of the substrate on film deformation. The unloading curves display an unusual slope at the maximum load, which diminishes as the penetration depth decreases. However, the Hertz model fit provides an accurate approximation to the experimental data under low load conditions. In light of this, we estimated the values of Young's modulus by using both models, considering them as the elastic and plastic limits. We also applied a correction factor to account for the substrate influence for both sets of samples. A frequently used model to quantify the substrate effect is that proposed by Doerner and Nix [42].

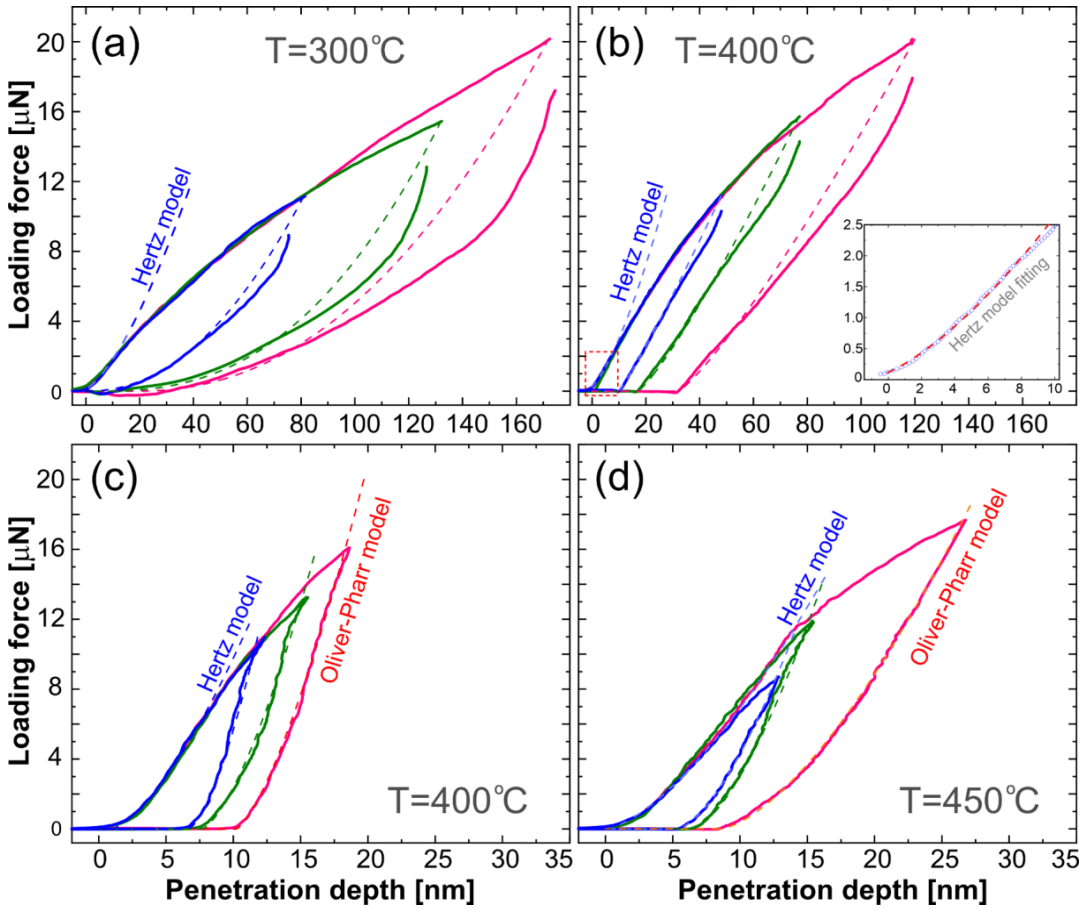

Fig. 2. Load penetration curves for the V_xO_y films annealed in the oxygen-reach (a, b) and in the inert atmosphere (c, d). Corresponding annealing temperatures are indicated. The Hertz model fit for the loading curve of the minimum loading force and the Oliver–Pharr model fit for the unloading curves are shown by the dashed curves. An enlarged part of the initial loading stage and the corresponding Hertz model fit are shown in (b).

According to this model, the substrate effect factor g is given by the following expression:

$$g = 1 - \left(1 - E_f^* / E_s^*\right)\left(1 - 0.8h/t\right), \quad (4)$$

where E_f^* is the reduced modulus of the film and E_s^* is the reduced modulus of the substrate, t is the film thickness.

The penetration depth is drastically reduced for films annealed in an argon atmosphere (the maximum loading forces are slightly lowered to avoid tip cantilever instability). Hertz and Oliver–Pharr models fit well at the same time.

Fig. 3 provides a summary of the measured hardness and Young's modulus values. Generally, the hardness of the oxygen-reach annealed samples is approximately an order of magnitude less than that of the argon-annealed samples. It equals 0.32 ± 0.02 GPa to 0.53 ± 0.04 GPa for films annealed in oxygen-reach atmosphere at 300 and 400 °C, while the hardness for the films annealed at the same temperatures in N_2 is 3.82 ± 0.42 GPa and 3.24 ± 0.23 GPa, respectively. Additionally, the data reveal an indentation size effect, as seen from the decrease in hardness with the increased indentation depth, when testing under varying loads (Fig. 2). This phenomenon is characteristic of materials that exhibit significant plasticity.

Fig. 3b depicts similar trends for the measured elastic modulus. As anticipated, a discrepancy exists between Young's modulus values derived from the Hertz model and the Oliver–Pharr model for both softer and harder films. For a soft material, more susceptible to plastic deformation, the Hertz model might overstate Young's modulus, since it doesn't account for energy dissipation through plastic deformation. On the other hand, the Oliver–Pharr model could provide more accurate estimation of the Young's modulus for soft materials, since it incorporates energy dissipation through plastic deformation. However, for hard materials, which are less prone to plastic deformation, the assumptions of the Hertz model may prove better fitting. Yet, should there be any plastic deformation, the Hertz model might underestimate Young's modulus. The Oliver–Pharr model might overestimate Young's modulus for hard materials, if there is substantial elastic recovery during unloading.

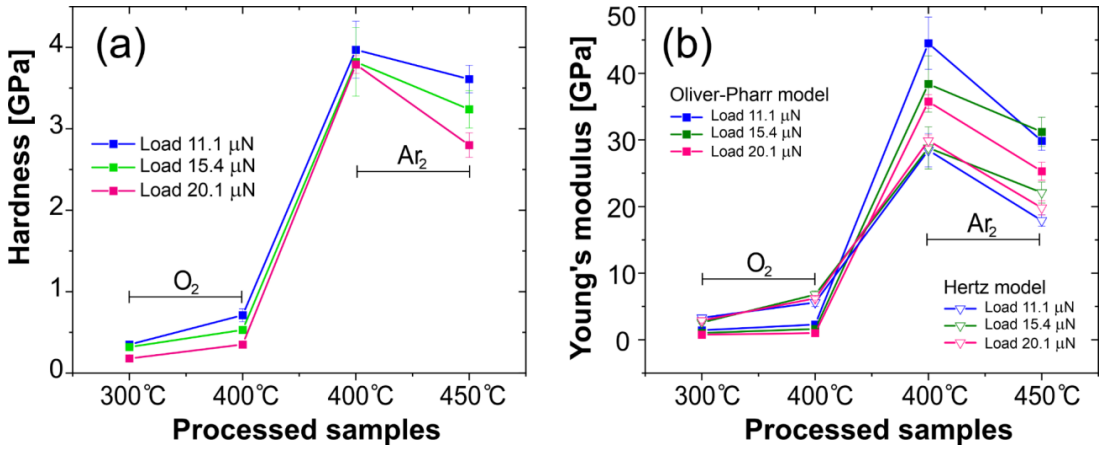

Fig. 3. Hardness (a) and Young's modulus (b) values of the annealed V_xO_y films. Young's modulus was determined using the elastic (Hertz model) and elastoplastic (Oliver–Pharr model) approaches. Horizontal bars indicate the oxygen-reach and argon atmospheres. The line is the guide to the eye only. (Color online)

For the purpose of this study, there's no need to employ more complex elasticity models; the estimates within the models currently used are sufficient to characterize the differences between the films. Thus, within the Hertz model, Young's modulus of the annealed films corresponds to the values of 1.43 ± 0.16, 2.28 ± 0.26, 44.50 ± 3.92, and 29.85 ± 1.41 GPa. The Oliver–Pharr model yields values of 3.30 ± 0.38, 5.60 ± 0.63, 28.45 ± 2.51, and 17.90 ± 0.84 GPa for the V_xO_y films annealed in oxygen-reach and argon atmospheres at temperatures of 300, 400 and 450 °C, respectively. The values are shown for the minimal load of 11 μN.

The mechanical properties of vanadium oxide films, specifically hardness and elasticity, are contingent on a multitude of factors. A discernibly higher hardness and Young's modulus are observed in vanadium oxide films after post-annealing in N_2 atmosphere, as opposed to oxygen-reach annealing. This enhancement can be attributed to alterations in phase composition, reduced oxidation levels, changes in grain size, decrease in the density of defects and dislocations, and reduction in phase interactions.

Notably different hardness of the films annealed in oxygen-reach and argon atmospheres correlate with different phase compositions of the films, ascertained from Raman and XRD studies discussed below. In particular, according to Raman data, VO_2 is the main phase of the films annealed in argon, with secondary phases of V_4O_9 and V_3O_7 (Fig. 4). Surprisingly, XRD gives for this sample 55% VO_2 and 45% V_4O_9. In the oxygen-reach annealed samples, VO_2 is the minority phase, according to XRD (28%), and the dominant part is nearly equally distributed between V_2O_5 (27%), V_4O_9 (22%) and V_3O_7 (23%). Notably, in the Raman spectra of the latter samples the vibrational peaks of VO_2 were not detected, indicating to much lower sensitivity of this method to the VO_2 phase in composite where other V_xO_y phases dominate. We may also make an assumption that the intensity of Raman scattering is not simply proportional to the total volume of the particular phase, but it may be noticeably higher, if the same amount of material forms large crystalline domains. Although the same dependence can be expected for XRD reflexes, the effect seems to be more pronounced in the Raman spectra. Therefore, with the assumption that the VO_2 phase in the oxygen-reach annealed samples is not only smaller in the net volume but exists in the form of smaller crystallites, this can be an additional reason for the lesser hardness of these films, as compared to the argon-annealed films, where the VO_2 phase has a large total volume and presumably larger domain size.

Moreover, the M1 phase of VO_2 is renowned for its distorted V–O–V bonds, which offer high covalency and thereby significantly contribute to the hardness of the material [43]. Hence, the higher amount of VO_2 phase in the N_2-annealed samples potentially explains the augmented hardness and Young's modulus observed. On the other hand, V_4O_9 (as well as V_3O_7) has a more complex crystal structure with weaker bonding, which can result in lower hardness. Even the smaller hardness difference between the films annealed at different temperatures in the same environment can similarly be explained by the smaller difference in the phase composition. Thus, the higher intensity of the secondary oxide Raman peaks for the film annealed in N_2 at 450 °C correlates with its slightly smaller hardness (3.24 GPa) as compared to that annealed at 400 °C (3.82 GPa). The relatively small decrease in hardness and modulus values upon N_2 annealing at 450 °C can be attributed to structural changes in the vanadium oxide film. This structural rearrangement leads to an increase in the RMS value together with the appearance of nanograins and surface depressions. These indicate a small general deterioration in the crystalline quality of the film and may contribute to the observed decrease in these mechanical properties.

Even in presence of the large portion of other V_xO_y phases, the VO_2 phases exhibit a pronounced

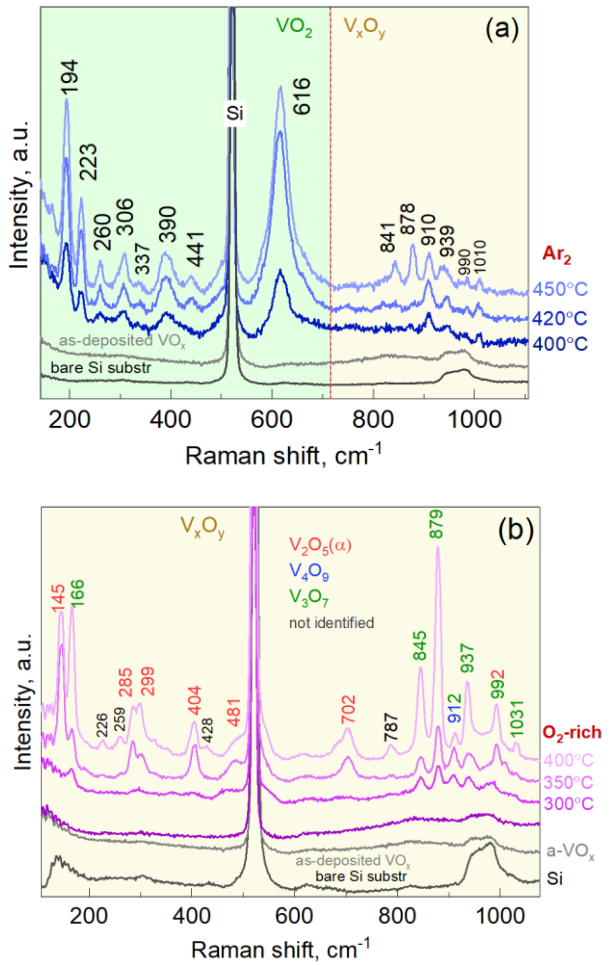

Fig. 4. Raman spectra of VO_x film deposited on Si at T_{sub} = 200 °C and annealed at different temperatures T_{ann} in N_2 (a) or oxygen-reach and argon ambient atmospheres (b). Spectra were measured at room temperature with λ_{exc} = 457 nm.

semiconductor-to-metal phase transition (SMT), with a characteristic transition temperature of 58 to 68 °C, which correlate with the previous works on similar thin films [30, 35–39]. A detailed study of the SMT transition in the films investigated in this work, as well as ascertaining the vibrational fingerprints of different V_xO_y phases in the Raman spectra will be reported elsewhere.

As previously noted, ion implantation, particularly with Ar^+ ions, is a technique with the potential to alter the mechanical properties of thin films. Implantation of Ar^+ ions into these films results in creation of lattice defects, including vacancies, interstitials and dislocations, due to the high-energy interactions between the ions and the film atoms. The presence of these defects can enhance the film hardness and elastic modulus. This enhancement could arise because the defects impede the movement of dislocations, which are the primary agents of plastic deformation. By restricting dislocation movement, the film resistance to deformation is heightened, leading to increased hardness. Additionally, the ion implantation can induce changes in the film residual stress. These stresses can affect the film adhesion to its substrate, with potential outcomes including delamination or cracking, if not adequately addressed. Moreover, the defects generated by Ar^+ implantation can act as initiation points for phase transitions or grain growth, both of which can have significant implications for the film mechanical and electronic properties.

Indeed, both X-ray diffraction and Raman spectroscopy reveal significant structural alterations in the Ar^+ implanted VO_x films. The intensity of the X-ray diffraction peaks diminished, and their angular positions shifted upon implantation. In addition, the full width at half maximum (FWHM) of the peaks increased, suggesting a relaxation of residual strains and the introduction of structural defects. In parallel, the intensity of all Raman bands dramatically decreased for the Ar-implanted samples. Notably, there were non-monotonic shifts in the A_g band at 616 cm^{-1}, which indicates an initial strain relaxation followed by an anisotropic redistribution of residual strains, since the implantation dose increased. Comprehensive findings from the XRD and Raman analyses of the implanted VO_x samples, along with their implications on MIT, will be published elsewhere.

The outcomes of nanoindentation, based on AFM, for the sample annealed in N_2 atmosphere and subsequently implanted up to a dose of $4.4 \cdot 10^{14}$ cm^{-2}, are shown in Fig. 5. Each case displays a series of three load-penetration curves, representing the uniformity of the nanomechanical properties across the VO_x film surface. The annealing temperature close to 300 °C does not adequately homogenize the vanadium oxide films produced by magnetron sputtering. In comparison with the data presented in Fig. 3, both the hardness and Young's modulus values are reduced (1.7, 12 GPa). Besides, there is a more noticeable variation in values when measurements are taken from different surface regions. The alignment between the loading and unloading segments of the indentation curves is not optimal. In contrast, the series of curves for the implanted film distinctly demonstrate an enhancement in both hardness and elastic modulus (2.8, 18 GPa), as well as a more consistent surface homogeneity.

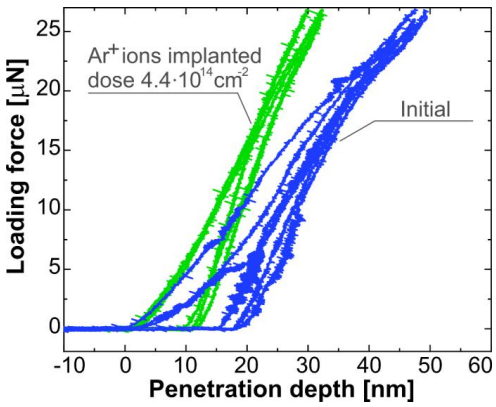

Fig. 5. Series of as-measured load-penetration curves obtained for the VO_x film annealed in N_2 at 300 °C and the film subsequently implanted with Ar^+ ions.

4. Conclusions

This work demonstrates the efficacy of AFM-based nanoindentation for sensitive quantification of phase composition and defect characterization in complex VO_x thin films. The high localization and force sensitivity enables clear delineation of variations in nanomechanical properties arising from different phase balances and ion beam induced damage in the functional oxide systems. The measured hardness and Young's modulus values exhibit extreme sensitivity to the relative amounts of VO_2 *versus* V_2O_5 and Magnéli phases, as well as more subtle changes in crystallinity and microstructure. Employing both the Hertz and Oliver–Pharr analytical models offers a comprehensive perspective on the nanomechanical behavior in both the elastic and elastoplastic domains. Furthermore, Ar^+ ion implantation is shown to enhance the hardness and elastic modulus of VO_x films by introducing lattice defects that impede plastic deformation.

Relating the measured nanomechanical trends to structural changes revealed *via* XRD and Raman spectroscopy provides critical insights into the structure-property relationships in this technologically relevant class of electronic materials. It was shown the AFM nanoindentation can serve as an express diagnostic tool for process control and optimization in VO_x thin film synthesis and modification for electronics applications. On a more fundamental level, this technique elucidates the intricate links between atomic structure evolution and nanoscale mechanical response in complex functional oxide systems, contributing to advancement of materials physics and mechanics.

Acknowledgements

The work was funded by the NAS of Ukraine programme "Support of the priority research directions" for 2023–2024, project # 4.4/23-П.

The authors are sincerely grateful to all defenders of Ukraine and emergency workers who made it possible for us to obtain results for this publication.

References

1. Huang F., Gong M., Tian S. *et al.* Controlling the crystalline orientation and textual morphologies of the VO_2 film and the effect on insulator–metal transition properties. *Jpn. J. Appl. Phys*. 2022. **61**. P. 085504. https://doi.org/10.35848/1347-4065/ac7c4c.
2. Cheng Y., Zhang Y., Fang C. *et al.* Regulation of morphology and structure of vanadium dioxide *via* a hydrothermal method for optimizing performances. *Ceram. Int.* 2022. **48**. P. 37423–37432. https://doi.org/10.1016/j.ceramint.2022.09.102.
3. Zeng W., Lai H., Chen T. *et al.* Size and crystallinity control of dispersed VO_2 particles for modulation of metal–insulator transition temperature and hysteresis. *CrystEngComm*. 2019. **21**. P. 5749–5756. https://doi.org/10.1039/C9CE01013K.
4. Zhang Y., Xiong W., Chen W. *et al.* Recent progress on vanadium dioxide nanostructures and devices: fabrication, properties, applications and perspectives. *Nanomaterials*. 2021. **11**, No 2. P. 338. https://doi.org/10.3390/nano11020338.
5. Yang Z., Ko C., Ramanathan S. Oxide electronics utilizing ultrafast metal-insulator transitions. *Annu. Rev. Mater. Res*. 2011. **41**. P. 337–367. https://doi.org/10.1146/annurev-matsci-062910-100347.
6. Chen S., Lust M., Ghalichechian N. Multiphysics simulation of hypersensitive microbolometer sensor using vanadium dioxide and air suspension for millimeter wave imaging. *Microsyst. Technol*. 2021. **27.** P. 2815–2822. https://doi.org/10.1007/s00542-020-05031-0.
7. Koita I., Tizei L.H.G., Blazit J.-D. *et al.* Metal/insulator transitions in V_2O_3 systems investigated at the nanoscale by spectromicroscopy techniques under cryo-conditions. *Microsc. Microanal*. 2023. **29**. P. 1691–1692. https://doi.org/10.1093/micmic/ozad067.870.
8. Hennen T., Bedau D., Rupp J.A.J. *et al.* Switching speed analysis and controlled oscillatory behavior of a Cr-doped V_2O_3 threshold switching device for memory selector and neuromorphic computing application, in: *2019 IEEE 11th International Memory Workshop (IMW), IEEE*. 2019. P. 1–4. https://doi.org/10.1109/IMW.2019.8739556.
9. Ling C., Zhao Z., Hu X. *et al.* W doping and voltage driven metal–insulator transition in VO_2 nano-films for smart switching devices. *ACS Appl. Nano Mater*. 2019. **2**. P. 6738–6746. https://doi.org/10.1021/acsanm.9b01640.
10. Sun G., Cao X., Long S. *et al.* Optical and electrical performance of thermochromic V_2O_3 thin film fabricated by magnetron sputtering. *Appl. Phys. Lett*. 2017. **111**. P. 053901. https://doi.org/10.1063/1.4997323.
11. Katzke H., Tolédano P., Depmeier W. Theory of morphotropic transformations in vanadium oxides. *Phys. Rev. B*. 2003. **68**. P. 024109. https://doi.org/10.1103/PhysRevB.68.024109.
12. Choi S., Son J., Oh J. *et al.* Sharp contrast in the electrical and optical properties of vanadium Wadsley (V_mO_{2m+1}, $m > 1$) epitaxial films selectively stabilized on (111)-oriented Y-stabilized ZrO_2. *Phys. Rev. Mater*. 2019. **3**. P. 063401. https://doi.org/10.1103/PhysRevMaterials.3.063401.
13. Schwingenschlögl U., Eyert V. The vanadium Magnéli phases V_nO_{2n-1}. *Ann. Phys*. 2004. **516**. P. 475–510. https://doi.org/10.1002/andp.20045160901.
14. Rupp J.A.J., Querré M., Kindsmüller A. *et al.* Different threshold and bipolar resistive switching mechanisms in reactively sputtered amorphous undoped and Cr-doped vanadium oxide thin films. *J. Appl. Phys*. 2018. **123**. P. 044502. https://doi.org/10.1063/1.5006145.
15. Shvets P., Maksimova K., Goikhman A. Correlation between Raman spectra and oxygen content in

amorphous vanadium oxides. *Phys. B: Condens. Matter*. 2021. **613**. P. 412995. https://doi.org/10.1016/j.physb.2021.412995.
16. Nandi S.K., Das S.K., Estherby C. *et al.* Understanding modes of negative differential resistance in amorphous and polycrystalline vanadium oxides. *J. Appl. Phys*. 2020. **128**. P. 244103. https://doi.org/10.1063/5.0027875.
17. Shen N., Chen S., Huang R. *et al.* Vanadium dioxide for thermochromic smart windows in ambient conditions. *Mater. Today Energy*. 2021. **21**. P. 100827. https://doi.org/10.1016/j.mtener.2021.100827.
18. Lamsal C., Ravindra N.M. Vanadium oxides for energy and security applications, in: *Spectroscopic Techniques for Security, Forensic and Environmental Applications.* Nova Science Publishers, Inc., 2014. P. 195–220.
19. Atanassova E., Lytvyn P., Dub S.N. *et al.* Nanomechanical properties of pure and doped Ta_2O_5 and the effect of microwave irradiation. *J. Phys. D: Appl. Phys*. 2012. **45**. P. 475304. https://doi.org/10.1088/0022-3727/45/47/475304.
20. Lytvyn P., Kuchuk A., Kondratenko S. *et al.* Strain-driven anomalous elastic properties of GeSn thin films. *Appl. Phys. Lett*. 2023. **123**. P. 022102. https://doi.org/10.1063/5.0149098.
21. Singh D., Viswanath B. In situ nanomechanical behaviour of coexisting insulating and metallic domains in VO_2 microbeams. *J. Mater. Sci*. 2017. **52**. P. 5589–5599. https://doi.org/10.1007/s10853-017-0792-4.
22. Guo H., Chen K., Oh Y. *et al.* Mechanics and dynamics of the strain-induced M1-M2 structural phase transition in individual VO_2 nanowires. *Nano Lett*. 2011. **11**. P. 3207–3213. https://doi.org/10.1021/nl201460v.
23. Sedlmayr A., Mönig R., Boles S.T. *et al.* Strain-induced phase transformation and piezoresistivity in VO_2 nanowires. *MRS Commun*. 2012. **2**. P. 41–45. https://doi.org/10.1557/mrc.2012.5.
24. Mazur M., Lubańska A., Domaradzki J. *et al.* Complex research on amorphous vanadium oxide thin films deposited by gas impulse magnetron sputtering. *Appl. Sci*. 2022. **12**. P. 8966. https://doi.org/10.3390/app12188966.
25. Birkhölzer Y.A., Sotthewes K., Gauquelin N. *et al.* High-strain-induced local modification of the electronic properties of VO_2 thin films. *ACS Appl. Electron. Mater*. 2022. **4**. P. 6020–6028. https://doi.org/10.1021/acsaelm.2c01176.
26. Fateh N., Fontalvo G.A., Mitterer C. Structural and mechanical properties of dc and pulsed dc reactive magnetron sputtered V_2O_5 films. *J. Phys. D: Appl. Phys*. 2007. **40**. P. 7716–7719. https://doi.org/10.1088/0022-3727/40/24/019.
27. Nieves C., Verbel C., Lysenko S. *et al.* Young's modulus of V_3O_5 thin films. *AIP Adv*. 2023. **13**. P. 085031. https://doi.org/10.1063/5.0159873.
28. Mogunov I.A., Lysenko S., Fedianin A.E. *et al.* Large non-thermal contribution to picosecond strain pulse generation using the photo-induced phase transition in VO_2. *Nat. Commun*. 2020. **11**. P. 1690. https://doi.org/10.1038/s41467-020-15372-z.
29. Jia Q., Grenzer J., He H. *et al.* 3D local manipulation of the metal–insulator transition behavior in VO_2 thin film by defect-induced lattice engineering. *Adv. Mater. Interfaces*. 2018. **5**, No 8. P. 1701268. https://doi.org/10.1002/admi.201701268.
30. Sabov T.M., Oberemok O.S., Dubikovskyi O.V. *et al.* Oxygen ion-beam modification of vanadium oxide films for reaching a high value of the resistance temperature coefficient. *SPQEO*. 2017. **20**. P. 153–158. https://doi.org/10.15407/spqeo20.02.153.
31. Mabakachaba B.M., Madiba I.G., Kennedy J. *et al.* Structural and electrical properties of Mg-doped vanadium dioxide thin films *via* room-temperature ion implantation. *Surf. Interfaces*. 2020. **20**. P. 100590. https://doi.org/10.1016/j.surfin.2020.100590.
32. Mei H., Koch A., Wan C. *et al.* Tuning carrier density and phase transitions in oxide semiconductors using focused ion beams. *Nanophotonics*. 2022. **11**. P. 3923–3932. https://doi.org/10.1515/nanoph-2022-0050.
33. Clifford C.A., Seah M.P. Quantification issues in the identification of nanoscale regions of homopolymers using modulus measurement via AFM nanoindentation. *Appl. Surf. Sci*. 2005. **252**. P. 1915–1933. https://doi.org/10.1016/j.apsusc.2005.08.090.
34. Chudoba T., Griepentrog M., Dück A. *et al.* Young's modulus measurements on ultra-thin coatings. *J. Mater. Res*. 2004. **19**. P. 301–314. https://doi.org/10.1557/jmr.2004.19.1.301.
35. Melnik V., Khatsevych I., Kladko V. *et al.* Low-temperature method for thermochromic high ordered VO_2 phase formation. *Mater. Lett*. 2012. **68**. P. 215–217. https://doi.org/10.1016/j.matlet.2011.10.075.
36. Liubchenko O., Kladko V., Melnik V. *et al.* Ar-implanted vanadium dioxide thin film with the reduced phase transition temperature. *Mater. Lett*. 2022. **314**. P. 131895. https://doi.org/10.1016/j.matlet.2022.131895.
37. Melnik V.P., Khatsevych I.M., Goltvyanskyi Yu.V. *et al.* Thermochromic properties of vanadium dioxide films obtained by magnetron sputtering. *Ukr. J. Phys*. 2022. **56**. P. 534. https://doi.org/10.15407/ujpe56.6.534.
38. Goltvyanskyi Yu., Khatsevych I., Kuchuk A. *et al.* Structural transformation and functional properties of vanadium oxide films after low-temperature annealing. *Thin Solid Films*. 2014. **564**. P. 179–185. https://doi.org/10.1016/j.tsf.2014.05.067.
39. Kladko V.P., Melnik V.P., Liubchenko O.I. *et al.* Phase transition in vanadium oxide films formed by multistep deposition. *SPQEO*. 2021. **24**. P. 362–371. https://doi.org/10.15407/spqeo24.04.362.

40. Kontomaris S.V., Malamou A. Hertz model or Oliver & Pharr analysis? Tutorial regarding AFM nanoindentation experiments on biological samples. *Mater. Res. Express*. 2020. **7**. P. 033001. https://doi.org/10.1088/2053-1591/ab79ce.
41. Pharr G.M., Oliver W.C. Measurement of thin film mechanical properties using nanoindentation. *MRS Bull*. 1992. **17**. P. 28–33. https://doi.org/10.1557/S0883769400041634.
42. Doerner M.F., Nix W.D. Stresses and deformation processes in thin films on substrates. *Crit. Rev. Solid State Mater. Sci*. 1988. **14**. P. 225–268. https://doi.org/10.1080/10408438808243734.
43. Reeswinkel T., Music D., Schneider J.M. Ab initio calculations of the structure and mechanical properties of vanadium oxides. *J. Phys.: Condens. Matter*. 2009. **21**. P. 145404. https://doi.org/10.1088/0953-8984/21/14/145404.

Authors and CV

Petro M. Lytvyn, Head of Department at the V. Lashkaryov Institute of Semiconductor Physics, NAS of Ukraine is renowned for his expertise in semiconductor materials and systems, scanning probe microscopy, and X-ray diagnostics. Holding a PhD in Physics and Mathematics, he has authored over 350 peer-reviewed publications, significantly advancing knowledge in his fields.
https://orcid.org/0000-0002-0131-9860

Volodymyr M. Dzhagan, Doctor of Sciences, Professor, Leading Researcher at the V. Lashkaryov Institute of Semiconductor Physics, author of over 200 publications. The area of scientific interests includes optical and vibrational properties of semiconductors, related nanostructures and composite materials. E-mail: dzhagan@isp.kiev.ua, https://orcid.org/0000-0002-7839-9862

Mykhailo Ya. Valakh, Professor, Doctor of Sciences, Corresponding Member of NAS of Ukraine, Principal Researcher at the V. Lashkaryov Institute of Semiconductor Physics, the author of more than 400 papers, 7 patents, 5 textbooks. The area of his scientific interests includes physics of semiconductors and dielectrics, optics and spectroscopy of solid state, material science for electronics, physics of nanostructures, optical diagnostics of materials. E-mail: mvalakh@gmail.com, https://orcid.org/0000-0003-3849-3499

Andrii A. Korchovyi, PhD in Physics and Mathematics. Senior Researcher at the Laboratory for scanning probe microscopy, V. Lashkaryov Institute of Semiconductor Physics. Authored over 80 publications. The area of his scientific interests includes atomic force microscopy, physical and chemical properties of semiconductor materials and nanostructures for modern micro- and nano-electronics. E-mail: akorchovyi@gmail.com, https://orcid.org/0000-0002-8848-7049

Oksana F. Isaieva, born in 1994, she defended his PhD thesis in Applied Physics and nanomaterials in 2021 at the V. Lashkaryov Institute of Semiconductor Physics and is currently a researcher at this Institute. Authored 14 publications, 4 patents. The area of her scientific interests includes nanocomposites sites and their syntheses, optical properties of nanomaterials. E-mail: oksana.isaieva@isp.kiev.ua, https://orcid.org/0000-0003-1313-5409

Oleksandr A. Stadnik, PhD in Physics and Mathematics, Deputy head of the Department Ion-beam Engineering and Structural Analysis at the V. Lashkaryov Institute of Semiconductor Physics. His research interests include molecular-beam epitaxy, analysis of the surface structure of semiconductor crystals, hetero- and nanosystems. E-mail: stadnik@isp.kiev.ua

Oleksandr A. Kulbachynskyi, PhD student at the Department of Ion-Beam Engineering at the V. Lashkaryov Institute of Semiconductor Physics. His main research activity is physics of thin films, chromogenic materials and SIMS analysis, ion implantation, analysis of thin film and multilayer structures. E-mail: s.kulbachynskyi@gmail.com, https://orcid.org/0000-0001-6657-5569

Olexandr Yo. Gudymenko, PhD in Physics and Mathematics, Researcher at the V. Lashkaryov Institute of Semiconductor Physics. Author of more than 60 publications. His research interests include: solid-state physics, dynamical theory of diffraction of radiation, X-ray optics, X-ray diffraction, analysis of semiconductor crystals, hetero- and nanosystems, XRD analysis of materials, X-ray reflectometry of thin films. E-mail: gudymen@ukr.net, https://orcid.org/0000-0002-5866-8084

Boris Romanyuk defended DrSc thesis in 1980 (Physics and Mathematics) at the V. Lashkaryov Institute of Semiconductor Physics, Head of the Department of Ion-Beam Engineering and Structural Analysis at the same institute. Authored more than 270 scientific publications. His research interests include: physics of semiconductors and dielectrics, ion-beam engineering and performed a wide range of studies of semiconductor structures. E-mail: romb@isp.kiev.ua, https://orcid.org/0000-0002-1688-7588

Viktor Melnik, Professor, acting director of the V. Lashkaryov Institute of Semiconductor Physics, NAS of Ukraine. He defended DrSci thesis in 2012 (Physics and Mathematics) at the V. Lashkaryov Institute of Semiconductor Physics. Author of more than 250 scientific publications. His main research activity is in the fields of ion-beam engineering and diagnostics.
E-mail: vp_mel@ukr.net,
https://orcid.org/0000-0002-8670-7415

Authors' contributions

Lytvyn P.M.: conceptualization, methodology, data curation, writing – original draft, visualization, writing – review & editing.
Dzhagan V.M.: writing – original draft, formal analysis, visualization, formal analysis, investigation, data curation.
Valakh M.Ya.: supervision, conceptualization, validation, formal analysis, project administration.
Korchovyi A.A.: investigation, formal analysis.
Isaieva O.F.: investigation, formal analysis.
Stadnik O.A.: investigation, formal analysis.
Kulbachynskyi O.A.: formal analysis, validation.
Gudymenko O.Yo.: investigation, formal analysis.
Romanyuk B.M.: funding acquisition, formal analysis.
Melnik V.P.: funding acquisition, supervision, formal analysis.

Наномеханічні властивості тонких плівок полікристалічного оксиду ванадію різного фазового складу

П.М. Литвин, В.М. Джаган, М.Я. Валах, А.А. Корчовий, О.Ф. Ісаєва, О.А. Стадник, О.А. Кульбачинський, О.Й. Гудименко, Б.М. Романюк, В.П. Мельник

Анотація. Тонкі плівки оксиду ванадію (VO_x) є багатообіцяючими матеріалами, котрі мають електричні, оптичні та механічні властивості, які можна коригувати, задаючи параметри структури при рості та за допомогою післяростових обробок. У цій роботі поєднано атомно-силову мікроскопію (АСМ) та наноіндентування, корельовані з рентгенівською дифрактометрією та раманівською спектроскопією, для дослідження складних зв'язків між впливом атмосфери відпалу плівок VO_x, їх фазовим складом і результуючими наномеханічними властивостями. З використанням алмазного вістря як нанорозмірного індентора, наномеханічні випробування проведені на плівках VO_x із систематичними варіаціями структури – від змішаних оксидів до плівок з домінуванням фази VO_2. Значення твердості та модуля пружності отримано з використанням аналітичного моделювання контакту зонд-поверхня в нанометровій шкалі розмірів. Між плівками різного фазового складу оксидів спостерігаються значні коливання механічних властивостей із підвищенням твердості та модуля пружності на порядок для плівок з переважанням фази VO_2 порівняно з оксидами іншої стехіометрії. Іонна імплантація додатково покращує наномеханічні параметри завдяки спрямованій інженерії дефектів. Порівняння тенденцій наномеханічних характеристик із детальними структурними та морфологічними параметрами дозволило проілюструвати зв'язки між структурою та механічними властивостями, що недоступно іншим методам. Широке використання запропонованого підходу в діагностиці матеріалів оксидів ванадію сприятиме оптимізації параметрів отримання та післяростових обробок для електронних застосувань, а також поглибленню розуміння фундаментальних взаємозв'язків наноструктурних особливостей та функціональності.

Ключові слова: полікристалічні тонкі плівки оксиду ванадію, фазовий склад, атомно-силова мікроскопія, наноіндентування, рентгенівська дифрактометрія, раманівська спектроскопія, іонна імплантація.